orientation of the S-C_β bond determines the spatial disposition of the sulfur lone pairs and thus influences the Fe-S bond. Similar conclusions have been drawn[28] from theoretical studies of Fe_2S_2 clusters. Noodleman and co-workers[28] have recently performed X_α calculations of an $[Fe_4S_4(SCH_3)_4]^{2-}$ complex and obtained for each site $\Delta E_Q = 1.08$, $\eta = 1.0$ and $\delta = 0.49$ mm/s, in excellent agreement with the results obtained here (Table III).

Acknowledgment. This work was supported by NSF Grant PCM 83-06964 and NIH Grant GM 32526.

Registry No. $(NBu_4)[Fe_4S_4(S\text{-}2,4,6\text{-}Pr_3C_6H_2)_4]$, 96455-61-7.

(38) Bair, R. A.; Goddard, W. A. *J. Am. Chem. Soc.* **1978**, *100*, 5669.

Contribution from the Thimann Laboratories, Department of Chemistry, University of California, Santa Cruz, California 95064, and Department of Chemistry, University of California, Berkeley, California 94720

Convenient Synthesis and Properties of $(R_4N)_2[Ni(SAr)_4]$ (Ar = C_6H_5, *p*-C_6H_4Cl, *p*-$C_6H_4CH_3$, and *m*-C_6H_4Cl) and the Structure of Tetraethylammonium Tetrakis(*p*-chlorobenzenethiolato)nickelate(II)

Steven G. Rosenfield, William H. Armstrong,† and Pradip K. Mascharak*

Received January 22, 1986

Reaction of $(Et_4N)_2NiCl_4$ and $(R_4N)(SAr)$ (Ar = C_6H_5, *p*-C_6H_4Cl, *m*-C_6H_4Cl, *p*-$C_6H_4CH_3$) in acetonitrile affords $(R_4N)_2[Ni(SAr)_4]$ in high yield. Syntheses of soluble nickel thiolates are not possible in protic solvents, where only insoluble polymeric materials are obtained. $(Et_4N)_2[Ni(S\text{-}p\text{-}C_6H_4Cl)_4]$ crystallizes in the monoclinic space group $P2_1/c$ with $a = 16.299$ (3) Å, $b = 15.464$ (3) Å, $c = 18.784$ (3) Å, $\beta = 109.17$ (1)°, and $Z = 4$. The structure, refined to $R = 3.5\%$, reveals a distorted tetrahedral arrangement of S atoms around Ni with the average Ni-S distance being 2.281 Å. Two S-Ni-S angles are ~90° while the average of the other four is close to 120°. Three of the four Ni-S vectors are coplanar with the corresponding phenyl rings. Unfavorable steric contacts between the ortho H atoms and Ni or S atoms do not allow either an idealized square-planar or a tetrahedral arrangement of thiolates around Ni. This together with the tendency of the Ni-S bonds to be coplanar with the phenyl rings gives rise to the observed distortion. The NMR spectra of $(R_4N)_2[Ni(SAr)_4]$ are assigned and discussed.

Recent EXAFS studies on active sites of hydrogenases[1] have estabilished sulfur ligation to nickel, and this finding has raised renewed interest in the chemistry of nickel thiolates. The discrete nickel-thiolato species with known structure include monomeric,[2] dimeric,[3a] linear[3b] and cyclic trimeric,[4] cyclic tetrameric,[5] cyclic hexameric,[6] and cyclic octameric[7] complexes. Since there is only one nickel atom present in the active sites of these enzymes, the structure and properties of monomeric nickel thiolates draw special attention. The only species reported in this category is $(Ph_4P)_2[Ni(SPh)_4]$;[2] $Ni(SR)_4^{2-}$ with R = alkyl have not been synthesized.[3b] The reported synthesis involves stepwise displacement of dithiosquarate (Dts^{2-}) ligands from $(Ph_4P)_2Ni(Dts)_2$ by PhS^- in hot acetonitrile. This procedure requires synthesis of dithiosquaric acid and the nickel complex $(Ph_4P)_2Ni(Dts)_2$. In our recent attempt to synthesize monomeric thiolato complexes of nickel from simple starting materials, we have discovered a straightforword, high-yield synthetic route to $[Ni(SAr)_4]^{2-}$ (Ar = C_6H_5, *p*-C_6H_4Cl, *p*-$C_6H_4CH_3$, *m*-C_6H_4Cl).[8] The structure of $(Et_4N)_2[Ni(S\text{-}p\text{-}C_6H_4Cl)_4]$ (**1**) has also been determined in order to reexamine the unusual distortions reported for $(Ph_4P)_2[Ni(SPh)_4]$.[2b,9] In addition to the synthetic and structural information, the NMR spectra and assignments of several arenethiolates of nickel are reported.

Experimental Section

Preparation of Compounds. The thiols were procured from Aldrich Chemical Co. $(Et_4N)_2NiCl_4$ was synthesized by following a standard procedure.[10] In the following preparations, degassed solvents were used and all manipulations were performed under an atmosphere of dry and pure dinitrogen.

Tetraalkylammonium Thiolates $(R_4N)(SR)$. Synthesis of $(Et_4N)(S\text{-}p\text{-}C_6H_4Cl)$ is a typical example. To a solution of 10 mmol of sodium methoxide (0.23 g sodium) in 60 mL of methanol were added an equivalent amount (1.45 g) of *p*-chlorobenzenethiol and, within 10 min, 2.1 g (10 mmol) of Et_4NBr. After the mixture was stirred for 1 h, the solvent was removed in vacuo. The oily residue was extracted with 80 mL of acetonitrile and the extract was filtered. The clear often pale yellow filtrate was used in the synthesis of the nickel complex.

$(Et_4N)_2[Ni(S\text{-}p\text{-}C_6H_4Cl)_4]$ (1). A 1.02-g (2.2-mmol) sample of $(Et_4N)_2NiCl_4$ was dissolved in 50 mL of acetonitrile, and this deep blue solution was slowly added with contant stirring to the tetraethylammonium *p*-chlorobenzenethiolate solution (10 mmol). The color rapidly turned dark red brown. After the addition was complete, the clear red brown mixture was stirred at room temperature for 1 h and then stored at -20 °C for 6 h. The dark crystals that separated during this period were filtered and recrystallized from 70 mL of warm (~40 °C) propionitrile. A 1.39-g (70%) yield of large blocks was collected by filtration, washed with 1:2 v/v acetonitrile/diethyl ether and dried in vacuo. Anal. Calcd for $C_{40}H_{56}N_2NiS_4Cl_4$: C, 53.74; H, 6.32; N, 3.13; Ni, 6.57; Cl, 15.88. Found: C, 53.83; H, 6.23; N, 3.10; Ni, 6.35; Cl, 15.86.

The mole ratios and amounts of reactants were the same in the following syntheses.

$(Et_4N)_2[Ni(SC_6H_5)_4]$. Tetraethylammonium benzenethiolate was extracted into propionitrile (40 mL). $(Et_4N)_2NiCl_4$ was dissolved in 40 mL of acetonitrile. Addition of nickel to the thiolate solution resulted in a deep red-brown mixture, which was filtered to remove a small amount

* To whom correspondence should be addressed at the University of California, Santa Cruz.
† University of California, Berkeley.

(1) Lindahl, P. A.; Kojima, N.; Hausinger, R. P.; Fox, J. A.; Teo, B.-K.; Walsh, C. T.; Orme-Johnson, W. H. *J. Am. Chem. Soc.* **1984**, *106*, 3062. Scott, R. A.; Wallin, S. A.; Czechowski, M.; DerVartanian, D. V.; LeGall, J.; Peck, H. D., Jr.; Moura, I. *J. Am. Chem. Soc.* **1984**, *106*, 6864.
(2) (a) Holah, D. G.; Coucouvanis, D. *J. Am. Chem. Soc.* **1975**, *97*, 6917. (b) Swenson, D.; Baenziger, N. C.; Coucouvanis, D. *J. Am. Chem. Soc.* **1978**, *100*, 1932.
(3) (a) Lane, R. W.; Ibers, J. A.; Frankel, R. B.; Papaefthymiou, G. C.; Holm, R. H. *J. Am. Chem. Soc.* **1977**, *99*, 84. (b) Watson, A. D.; Rao, C. P.; Dorfman, J. R.; Holm, R. H. *Inorg. Chem.* **1985**, *24*, 2820.
(4) Tremel, W.; Krebs, B.; Henkel, G. *Inorg. Chim. Acta* **1983**, *80*, L31. Henkel, G.; Tremel, W.; Krebs, B. *Angew. Chem., Int. Ed. Engl.* **1983**, *22*, 319
(5) Gaete, W.; Ros, J.; Solans, X.; Font-Altaba, M.; Briansó, J. L. *Inorg. Chem.* **1984**, *23*, 39.
(6) Woodward, P.; Dahl, L. F.; Abel, E. W.; Crosse, B. C. *J. Am. Chem. Soc.* **1965**, *87*, 5251.
(7) Dance, I. G.; Scudder, M. L.; Secomb, R. *Inorg. Chem.* **1985**, *24*, 1201.
(8) As the manuscript for this paper approached completion, a brief report on a similar preparative route to $(Et_4N)_2[Ni(SPh)_4]$ appeared: Yamamaura, T.; Miyamae, H.; Katayama, Y.; Sasaki, Y. *Chem. Lett.* 1985, 269.
(9) Coucouvanis, D.; Swenson, D.; Baenziger, N. C.; Murphy, C.; Holah, D. G.; Sfarnas, N.; Simopoulos, A.; Kostikas, A. *J. Am. Chem. Soc.* **1981**, *103*, 3350.
(10) Gill, N. S.; Taylor, F. B. *Inorg. Synth.* **1967**, *9*, 136.

0020-1669/86/1325-3014$01.50/0

Table I. Summary of Crystal Data, Intensity Collection, and Structure Refinement Parameters for $(Et_4N)_2[Ni(S\text{-}p\text{-}C_6H_4Cl)_4]$[a]

formula	$C_{40}H_{56}Cl_4N_2NiS_4$
fw	893.68
space group	$P2_1/c$
a, Å	16.299 (3)
b, Å	15.464 (3)
c, Å	18.784 (2)
β, deg	109.17 (1)
V, Å^3	4471.7
Z	4
D_{calcd}, g cm^{-3}	1.327
D_{obsd}, g cm^{-3} [b]	1.325
crystal dimens, mm	0.25 × 0.25 × 0.38
radiation	Mo Kα (0.71073 Å)
abs coeff, cm^{-1}	8.85
data collcd	$3° \le 2\theta \le 45°$; $+h,+k,\pm l$
total no. of unique data collcd	5821
no. of unique data with $I > 3\sigma(I)$	3684
no. of params	477
R, %	3.5
R_w, %	4.0
GOF	1.58

[a] Data were collected at 22 °C. [b] Determined by flotation in CCl_4/cyclohexane.

of white solid and then stored at −20 °C for 24 h. The microcrystalline solid thus separated was recrystallized from 40 mL of warm (~50 °C) propionitrile. The dark prism-shaped crystals (1.31 g, 78%) were collected by filtration, washed with 1:4 v/v acetonitrile/diethyl ether, and dried in vacuo. Anal. Calcd for $C_{40}H_{60}N_2NiS_4$: C, 63.54; H, 8.01; N, 3.71; Ni, 7.77. Found: C, 63.34; H, 8.15; N, 3.63; Ni, 7.52.

$(Ph_4P)_2[Ni(SC_6H_5)_4]$. Addition of $(Et_4N)_2NiCl_4$ to the thiolate (Ph_4P^+ salt) in acetonitrile brought about the blue to dark red-brown color change and immediate precipitation of a microcrystalline solid. The product was recrystallized from 60 mL of hot (~ 70 °C) acetonitrile to afford 2.50 g (95%) of dark brown blocks. Anal. Calcd for $C_{72}H_{60}P_2NiS_4$: C, 73.64; H, 5.15; Ni, 5.00. Found: C, 73.72; H, 5.11; Ni, 4.92.

$(Et_4N)_2[Ni(S\text{-}m\text{-}C_6H_4Cl)_4]$. The reaction was performed in acetonitrile. However, after the addition of nickel to thiolate, the volume of the deep red-brown mixture was reduced to ~50 mL and it was then stored at −20 °C for 20 h. The dark crystals were collected by filtration and recrystallized from 50 mL of warm (~50 °C) propionitrile. A 1.2-g (61%) yield of large blocks was collected. Anal. Calcd for $C_{40}H_{56}N_2NiS_4Cl_4$: C, 53.74, H, 6.32; N, 3.13; Ni, 6.60; Cl, 15.88. Found: C, 53.65; H, 6.27; N, 3.20; Ni, 6.54; Cl, 16.05.

$(Et_4N)_2[Ni(S\text{-}p\text{-}C_6H_4CH_3)_4]$. After the addition of nickel to thiolate in acetonitrile, the volume of the deep red mixture (130 mL) was reduced to ~50 mL, and it was then stored at −20 °C for 20 h. The dark microcrystalline solid thus separated was collected by filtration. Recrystallization from 50 mL of warm (~50 °C) propionitrile afforded 1.45 g (81%) of dark needles. Anal. Calcd for $C_{44}H_{68}N_2NiS_4$: C, 65.07; H, 8.45; N, 3.45; Ni, 7.23. Found: C, 64.98% H, 8.40; N, 3.31; Ni, 7.43.

Physical Measurements. ^1H NMR spectra were recorded on a General Electric 300-MHz GN-300 spectrometer. Following the usual convention for the spectra of paramagnetic molecules, we designated chemical shifts which are upfield and downfield of the Me_4Si reference as positive and negative, respectively. Solution magnetic susceptibilities were determined by the conventional NMR method[11] using Me_4Si, and reference shift differences were measured to ±0.2 Hz, using 15–30 mM solutions in CD_3CN and $(CD_3)_2SO$. All susceptibility data were corrected for diamagnetism. Absorption spectra were recorded on a Perkin-Elmer Lambda 9 spectrophotometer. Microanalyses were performed by Galbraith Laboratories, Inc., TN. Nickel was estimated gravimetrically with dimethylglyoxime.

X-ray Data Collection and Reduction. Dark red crystals were grown by cooling a propionitrile solution of **1**. A suitable crystal was wedged into a glass capillary and sealed under an atmosphere of dinitrogen. The diffractometer data and precession photographs showed the crystal to belong to the monoclinic crystal system with systematic absences $h0l$ ($h + l = 2n + 1$) and $0k0$ ($k = 2n + 1$), consistent only with the space group $P2_1/c$. The orientation matrix and unit cell parameters were determined from the setting angles of 24 reflections with $2\theta \ge 27.5°$. The intensities

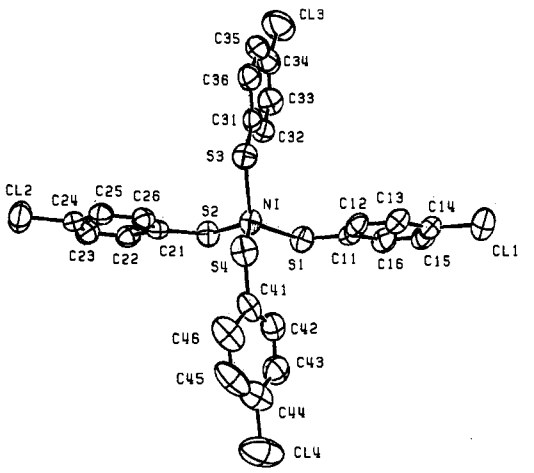

Figure 1. ORTEP drawing of $[Ni(S\text{-}p\text{-}C_6H_4Cl)_4]^{2-}$ showing 50% probability ellipsoids and the atom-labeling scheme. Hydrogen atoms are omitted for clarity.

of three standard reflections, monitored after every 1 h, were constant throughout the data collection. The positions of three orientation standards were checked after every 200 reflections; no reorientation was required. Owing to (i) the relatively small absorption coefficient, (ii) the very irregular shape of the crysal, and (iii) the small variations observed in azimuthal scans for four reflections with 2θ between 11 and 26°, no absorption correction was applied to the diffraction data. Further details of the data collection and reduction are given in Table I and in ref 12–19.

Solution and Refinement of the Structure. The direct-methods program MULTAN[20] revealed trial positions for the Ni, four Cl, and four S atoms. The remaining non-hydrogen atoms were located in subsequent difference Fourier maps. Calculated fixed contributions from hydrogen atoms (d(C–H) = 0.95 Å) with isotropic thermal parameters set at 1.2 times the isotropic equivalent of the bonded carbon atom were included in the final cycles of refinement. Positions for the methylene groups of the second counterion were disordered. The two positions for a given methylene group were estimated to be occupied in a 75:25 ratio. When allowed to refine, the ratio converged to 0.754:0.246 for the occupancies of the two positions. The structure was refined by using anisotropic thermal parameters for all non-hydrogen atoms (except for the lesser occupied methylene carbon atoms in the disordered counterion). Full-matrix least-squares refinement converged to the R indices listed in Table

(11) Evans, D. F. *J. Chem. Soc.* **1959**, 2003. Phillips, W. D.; Poe, M. *Methods Enzymol.* **1972**, *24*, 304.

(12) Roof, R. B. "A Theoretical Extension of the Reduced-Cell Concept in Crystallography"; Publication LA-4038; Los Alamos Scientific Laboratory: Los Alamos, NM, 1969.

(13) All calculations were performed with a PDP 11/60 equipped with 128 kilowords of memory, twin RK07 20 MByte disk drives, a Versatec printer/plotter, and a TU10 tape drive using locally modified Enraf-Nonius SDP software operating under RSX-11M.

(14) *Structure Determination Package User's Guide*; Molecular Structure Corp.: College Station, TX.

(15) The data reduction formulas are $F_0^2 = (\omega(C - 2B)/(Lp))$, $F_0 = (F_0^2)^{1/2}$, $\sigma_0(F_0^2) = \omega(C + 4B)^{1/2}/(Lp)$, and $\sigma_0(F_0) = \sigma_0(F_0^2)/2F_0$, where C is the total count in the scan, B is the sum of the two background counts, ω is the scan speed in deg/min, and $1/(Lp) = (\sin 2\theta)(1 + \cos^2 2\theta_m)/(1 + \cos^2 \theta_m - \sin^2 2\theta)$ is the correction for Lorentz and polarization effects for reflection with scattering angle 2θ and radiation monochromatized with a 50% perfect single-crystal monochromator with scattering angle $2\theta_m$.

(16) $R = (\sum||F_o| - |F_c||)/\sum|F_o|$, $R_w = [(\sum w(|F_o| - |F_c|)^2)/\sum wF_o^2]^{1/2}$, and GOF = $[(\sum w(|F_o| - |F_c|)^2)/(n_o - n_v)]^{1/2}$ where n_o is the number of observations and n_v is the number of variable parameters, and the weights w are given by $w = 4F_o^2/\sigma^2(F_o^2)$ and $\sigma^2(F_o^2) = \sigma_o^2(F_o^2) + (pF^2)^2$, where p is the factor used to lower the weight of intense reflections.

(17) Atomic scattering factors are from: Cromer, D. T.; Weber, J. T. *International Tables for X-ray Crystallography*; Kynoch: Birmingham, England, 1974; Vol. IV, Table 2.2B. Cromer, D. T. *Ibid.*; Table 2.3.1.

(18) Instrumentation at the University of California, Berkeley, Chemistry Department X-ray Crystallography Facility (CHEXRAY) consists of two Enraf-Nonius CAD-4 diffractometers, one controlled by a DEC PDP 8/a with a RK05 disk and the other by a DEC PDP 8/e with an RL01 disk. Both use Enraf-Nonius software as described in: *CAD-4 Operation Manual*; Enraf-Nonius: Delft, Amsterdam, The Netherlands, 1977 (updated in Jan 1980).

(19) Johnson, C. K. Report ORNL-3794; Oak Ridge National Laboratory: Oak Ridge, TN 1965.

(20) Germain, G.; Main, P.; Woolfson, M. M. *Acta Crystallogr., Sect. A: Cryst. Phys., Diffr., Gen. Theor. Crystallogr.* **1971**, *A27*, 368.

Table II. Positional and Thermal Parameters and Their Estimated Standard Deviations for $(Et_4N)_2[Ni(S\text{-}p\text{-}C_6H_4Cl)_4]$

atom	x	y	z	B,[a] Å²
Ni	0.27436 (3)	0.01066 (3)	0.52341 (3)	4.07 (1)
Cl1	−0.09143 (8)	−0.03537 (9)	0.16052 (7)	7.38 (4)
Cl2	0.68665 (8)	0.06762 (9)	0.84658 (7)	7.09 (4)
Cl3	0.0695 (1)	0.4253 (1)	0.58317 (9)	9.19 (5)
Cl4	0.3694 (1)	−0.4481 (1)	0.45676 (8)	10.85 (5)
S1	0.13729 (6)	−0.04043 (8)	0.50270 (6)	4.67 (3)
S2	0.30102 (6)	−0.01176 (8)	0.64905 (5)	4.55 (3)
S3	0.30087 (7)	0.14927 (8)	0.49348 (6)	4.82 (3)
S4	0.36006 (7)	−0.04061 (9)	0.45906 (6)	5.50 (3)
N1	0.1040 (2)	0.7313 (2)	0.1929 (2)	4.33 (8)
N2	0.6178 (2)	0.7210 (2)	0.2200 (2)	3.65 (8)
C11	0.0767 (2)	−0.0378 (2)	0.4063 (2)	4.0 (1)
C12	0.1103 (2)	−0.0150 (3)	0.3504 (2)	4.1 (1)
C13	0.0590 (2)	−0.0130 (3)	0.2755 (2)	4.6 (1)
C14	−0.0266 (3)	−0.0355 (3)	0.2559 (2)	4.7 (1)
C15	−0.0626 (3)	−0.0578 (3)	0.3097 (3)	5.4 (1)
C16	−0.0114 (2)	−0.0587 (3)	0.3843 (2)	4.9 (1)
C21	0.4096 (2)	0.0102 (2)	0.7010 (2)	3.63 (9)
C22	0.4373 (3)	−0.0006 (3)	0.7792 (2)	4.4 (1)
C23	0.5212 (3)	0.0167 (3)	0.8235 (2)	4.8 (1)
C24	0.5796 (3)	0.0463 (3)	0.7903 (2)	4.3 (1)
C25	0.5554 (2)	0.0573 (3)	0.7134 (2)	4.2 (1)
C26	0.4711 (2)	0.0386 (2)	0.6693 (2)	3.90 (9)
C31	0.2380 (3)	0.2242 (3)	0.5232 (2)	4.3 (1)
C32	0.1775 (3)	0.2014 (3)	0.5577 (2)	4.8 (1)
C33	0.1265 (3)	0.2628 (3)	0.5760 (2)	5.7 (1)
C34	0.1358 (3)	0.3483 (3)	0.5608 (2)	5.9 (1)
C35	0.1958 (3)	0.3736 (3)	0.5287 (2)	5.9 (1)
C36	0.2465 (3)	0.3119 (3)	0.5106 (2)	5.4 (1)
C41	0.3603 (2)	−0.1543 (3)	0.4602 (2)	4.7 (1)
C42	0.2914 (3)	−0.2043 (3)	0.4646 (2)	5.1 (1)
C43	0.2946 (3)	−0.2934 (3)	0.4647 (2)	6.1 (1)
C44	0.3666 (3)	−0.3344 (3)	0.4594 (2)	7.1 (1)
C45	0.4357 (3)	−0.2883 (3)	0.4551 (2)	7.6 (1)
C46	0.4346 (3)	−0.1985 (3)	0.4565 (2)	6.7 (1)
C51	0.0252 (3)	0.6760 (3)	0.1529 (3)	5.9 (1)
C52	−0.0617 (3)	0.7196 (3)	0.1370 (3)	7.9 (2)
C53	0.1096 (3)	0.8081 (3)	0.1448 (3)	5.9 (1)
C54	0.1224 (4)	0.7855 (4)	0.0709 (3)	8.9 (2)
C55	0.1825 (3)	0.6743 (3)	0.2086 (3)	6.0 (1)
C56	0.2687 (3)	0.7164 (3)	0.2477 (3)	6.8 (1)
C57	0.0961 (3)	0.7683 (3)	0.2645 (3)	5.7 (1)
C58	0.0826 (3)	0.7041 (4)	0.3197 (3)	7.6 (2)
C61	0.5416 (3)	0.6666 (3)	0.1775 (3)	4.4 (1)
C61A	0.531 (1)	0.763 (1)	0.170 (1)	5.5 (4)*
C62	0.4561 (3)	0.7119 (3)	0.1481 (3)	6.4 (1)
C63	0.6420 (3)	0.7795 (4)	0.1665 (3)	4.8 (1)
C63A	0.682 (1)	0.795 (1)	0.245 (1)	6.3 (5)*
C64	0.7180 (3)	0.8339 (4)	0.1946 (3)	8.8 (2)
C65A	0.640 (1)	0.652 (1)	0.1722 (9)	5.2 (4)*
C65	0.6925 (3)	0.6605 (4)	0.2626 (3)	5.1 (2)
C66	0.7296 (3)	0.6086 (3)	0.2142 (2)	7.1 (1)
C67A	0.606 (1)	0.679 (1)	0.2884 (9)	4.7 (4)*
C67	0.5985 (3)	0.7752 (3)	0.2795 (3)	4.0 (1)
C68	0.5622 (3)	0.7291 (3)	0.3316 (2)	5.4 (1)

[a] Starred values denote isotropically refined atoms. Values for anisotropically refined atoms are given in the form of the isotropic equivalent thermal parameter defined as: $(4/3)[a^2B_{11} + b^2B_{22} + c^2B_{33} + ab(\cos\gamma)B_{12} + ac(\cos\beta)B_{13} + bc(\cos\alpha)B_{23}]$. Atoms C61A, C63A, C65A, and C67A are the partially occupied positions (24.6%) corresponding to atoms C61, C63, C65, and C67, respectively. Atoms N1, N2 and C51–C68 constitute the cations.

I. The largest ratio of parameter shift to estimated standard deviation in the final cycle of refinement was 0.01, and the largest peak on the final difference Fourier map was 0.65 e/Å³ in the proximity of C46. Final positional parameters and isotropic equivalent thermal parameters are given in Table II. A list of angles and distances is provided in Table III. Anisotropic thermal parameters, positional and thermal parameters for hydrogen atoms, and observed and calculated structure factors are presented as supplementary material.

Results and Discussion

Two important findings led to the successful syntheses of arenethiolates of nickel from simple starting materials. The first one is the choice of solvent. Mixing of nickel salts[21] and thiolates in any order and ratio in methanol or ethanol yielded insoluble polymeric material(s). Even addition of ca. 10% alcohol to an acetonitrile solution of the arenethiolates caused precipitation of insoluble polymer(s) within a few minutes. The mechanism of the polymerization in presence of protic solvent has not been studied. It is noted that the syntheses of $(Ph_4P)_2[Ni(SPh)_4]$[2a] and $(Me_4N)_2[Ni_2(SEt)_6]$[3b] have also been achieved in acetonitrile. Thus the choice of a nonprotic solvent in the synthesis of thiolato complexes of nickel seems to be a general one. The second important factor is the presence of excess thiolate throughout the entire stage of mixing. The desired order of addition is nickel to thiolate. If the order is reversed, even in acetonitrile solution, only polymeric material is obtained. It is expected that these two synthetic strategies will be extremely helpful in future attempts to isolate discrete thiolato complexes of nickel.

Table III. Selected Distances (Å) and Angles (deg) in $[Ni(S\text{-}p\text{-}C_6H_4Cl)_4]^{2-}$ [a]

Ni–S1	2.279 (1)	S1–Ni–S2	88.11 (3)
Ni–S2	2.281 (1)	S1–Ni–S3	122.36 (4)
Ni–S3	2.293 (1)	S1–Ni–S4	121.89 (4)
Ni–S4	2.269 (1)	S2–Ni–S3	114.11 (4)
		S2–Ni–S4	123.81 (4)
		S3–Ni–S4	89.86 (4)
C14–Cl1	1.756 (4)	Ni–S1–C11	110.9 (1)
C24–Cl2	1.749 (3)	Ni–S2–C21	111.2 (1)
C34–Cl3	1.750 (4)	Ni–S3–C31	111.3 (1)
C44–Cl4	1.761 (5)	Ni–S4–C41	110.0 (1)
C11–S1	1.755 (3)	(Ni–S1)–(ring 1)[b]	5.4
C21–S2	1.751 (3)	(Ni–S2)–(ring 2)	0.2
C31–S3	1.755 (4)	(Ni–S3)–(ring 3)	0.3
C41–S4	1.758 (4)	(Ni–S4)–(ring 4)	26.7
1–3[c]	62.4	3–4	67.0
1–4	50.6	3–5	76.1
1–5	55.1	4–6	68.3
1–6	52.1	5–6	72.8
2–3	51.4	3–6	72.1
2–4	51.0	4–5	67.4
2–5	52.5		
2–6	60.7	1–2	94.7

[a] See Figure 1 for anion atom-labeling scheme. [b] Angle between the Ni–S1 vector and the least-squares plane of the phenyl ring bound to S1. [c] Dihedral angles between planes. The planes are numbered as follows: 1, S1–Ni–S2; 2, S3–Ni–S4; 3, S1–Ni–S3; 4, S1–Ni–S4; 5, S2–Ni–S3; 6, S2–Ni–S4.

Structure of $(Et_4N)_2[Ni(S\text{-}p\text{-}C_6H_4Cl)_4]$. (1). The crystal structure consists of discrete cations and anions. Structural features of the cations are unexceptional and are not discussed. The structure of the anion is shown in Figure 1. The arrangement of four sulfur atoms around nickel is distorted tetrahedral. In general, Ni(II) complexes with four coordinated sulfur atoms are square planar.[3b,22] Examples of the few tetrahedral NiS_4 complexes include $(Ph_4P)_2[Ni(SC_6H_5)_4]^2$ (**2**) and $[SP(CH_3)_2N(CH_3)_2PS]_2Ni$ (**3**).[22,23] The average Ni–S distance in **1** (2.281 Å) is very similar to those reported for **2** (2.288 Å) and **3** (2.282 Å). This Ni–S distance is considerably shorter than the average Ni–S bond length (2.444 Å) in the octahedral complex $[Ni(bpy)_2(SC_6H_5)_2]\cdot D_2O$.[24] The distortion from tetrahedral symmetry in **1** is such that two of the S–Ni–S angles are nearly 90° while the average of the other four is close to 120° (Table III). For the purpose of discussion, we consider an idealized geometry in which (i) all of the Ni–S distances are equivalent, (ii) two of the S–Ni–S

(21) The sources of nickel that have been tried in these attempts include $NiCl_2\cdot 2H_2O$, $(Et_4N)_2NiCl_4$, $(PPh_3)_2NiCl_2$, $Ni(CH_3COOH)_6(BF_4)_2$, and $Ni(dtc)_2$ (dtc = dithiocarbamate, $(C_6H_5)_2NCS_2^-$).
(22) Churchill, M. R.; Cooke, J.; Fennessey, J. P.; Wormald, J. *Inorg. Chem.* **1971**, *10*, 1031 and references therein.
(23) Davison, A.; Switkes, E. S. *Inorg. Chem.* **1971**, *10*, 837.
(24) Osakada, K.; Yamamoto, T.; Yamamoto, A.; Takenaka, A.; Sasada, Y. *Acta Crystallogr. Sect. C: Cryst. Struct. Commun.* **1984**, *C40*, 85.

Table IV. ^1H NMR Chemical Shifts (ppm, ~298 K) of $[Ni(SAr)_4]^{2-}$

compd	solvent	hydrogen ortho	hydrogen meta	hydrogen para
$(Et_4N)_2[Ni(SC_6H_5)_4]$	CD_3CN	−1.91 (2)[a,b]	−21.67 (2)	12.46 (1)
	$(CD_3)_2SO$	−2.65 (2)	−21.47 (2)	11.78 (1)
$(Ph_4P)_2[Ni(SC_6H_5)_4]$	$(CD_3)_2SO$[c]	−2.76 (2)	−21.50 (2)	11.80 (1)
$(Et_4N)_2[Ni(S\text{-}p\text{-}C_6H_4Cl)_4]$	CD_3CN	−1.92 (1)[a]	−22.28 (1)	
	$(CD_3)_2SO$	−0.73 (1)	−22.01 (1)	
$(Et_4N)_2[Ni(S\text{-}m\text{-}C_6H_4Cl)_4]$	CD_3CN	−1.79 (1), 0.52 (1)	−22.07 (1)	13.88 (1)
	$(CD_3)_2SO$	−1.42 (1), 0.40 (1)	−21.51 (1)	13.66 (1)
$(Et_4N)_2[Ni(S\text{-}p\text{-}C_6H_4CH_3)_4]$	CD_3CN	−2.39 (2)	−21.81 (2)	−26.39 (3)[d]
	$(CD_3)_2SO$	−1.69 (2)	−21.62 (2)	−25.87 (3)[d]

[a] Along with CH_3CN signal. [b] Relative intensity of the peak in parentheses. [c] Compound not sufficiently soluble in CD_3CN. [d] $p\text{-}CH_3$ signal.

angles are 90°, and (iii) the dihedral angle between these two coordination planes (S1–Ni–S2, S3–Ni–S4 in our case) is 90°. For such an idealized geometry, the calculated value for the four nonorthogonal S–Ni–S angles is 120°, which is in good agreement with the relatively tight grouping around an average value of 120.5° observed for **1**. Further evidence for the congruence between the structure of **1** and the idealized geometry considered here arises from a comparison of dihedral angles. In the idealized D_{2d} structure, there are eight dihedral angles with values of $\cos^{-1}(1/3^{1/2}) = 54.74°$ and six angles of $\cos^{-1}(1/3) = 70.53°$ in addition to one 90° dihedral angle. In **1**, we observe eight dihedral angles closely spaced around an average of 54.5° and a quite distinct set of six distributed about an average of 70.6°. Thus **1** closely approaches the idealized situation presented above. A similar distortion was observed for $(Ph_4P)_2[Ni(SC_6H_5)_4]$ and a number of other isomorphous $(Ph_4P)_2[M(SC_6H_5)_4]$ structures (M = Co, Zn, Cd) and was originally attributed to crystal packing forces.[2b] Since the distortion persists in our case where both the counterion and the thiolate are changed, it is unlikely that the distortion is brought about by such packing forces. It was recognized previously[25] that this kind of distortion apparently results from the tendency of a Ni–S bond to lie in the plane of the phenyl ring which is attached to the sulfur atom. In **1**, this feature is evident from inspection of Figure 1 and from the calculated angles between the least-squares planes of the phenyl rings and the adjacent Ni–S vectors (Table III). Three of the four angles are close to 0° while the Ni–S4 vector lies well out of the plane of the corresponding phenyl ring. A consequence of this structural feature is that neither ideal square-planar nor tetrahedral geometry is permissible owing to sterically unfavorable contacts that would result principally between phenyl ortho hydrogen atoms and the nickel and sulfur atoms.[9,25] The overriding factor that determines the geometry around nickel appears to be the stabilization that is gained by allowing the Ni–S vectors to be coplanar with the bonded phenyl ring.

The high solubility of $(Et_4N)_2[Ni(SAr)_4]$ in various solvents allowed assignments of the ^1H NMR spectra of these complexes. The various peak positions and their relative intensities are listed in Table IV. Like other nickel(II) compounds,[26] these arenethiolates give rise to extremely sharp (Figure 2) paramagnetically shifted resonances. The only exceptions are the peaks due to ortho hydrogens, which are somewhat broadened due to their proximity to the paramagnetic ($S = 1$) metal center. The alternate sign pattern of ortho, meta, and para hydrogen peaks around their diamagnetic positions is an evidence for dominant paramagnetic contact interaction through π spin delocalization.[26,27] When the para hydrogen was replaced by a CH_3 group, the sign of the isotropic shift reversed (Table IV), further demonstrating delocalization of spin via the aromatic π system. Substitution of meta and para hydrogen atoms with Cl and CH_3 groups in these complexes clearly identified the corresponding resonances in their

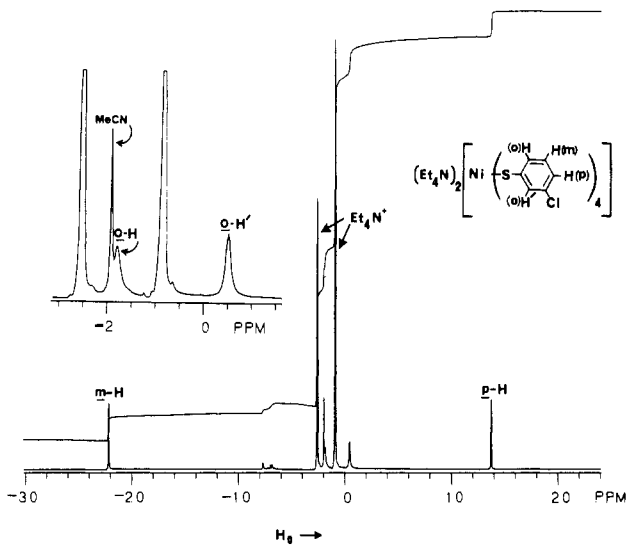

Figure 2. ^1H NMR spectrum (300 MHz, 298 K) of a 17.5 mM solution of $(Et_4N)_2[Ni(S\text{-}m\text{-}C_6H_4Cl)_4]$ in CD_3CN. Signal assignments are indicated.

NMR spectra (Table IV). The peak positions for meta and para hydrogens are relatively insensitive to change of solvent. This is, however, not true for ortho hydrogen resonances which shifted ca. 1 ppm when the solvent was changed from CD_3CN to $(CD_3)_2SO$. In $[Ni(S\text{-}m\text{-}C_6H_4Cl)_4]^{2-}$, two ortho hydrogen atoms are not equivalent and indeed two resonances were recorded (Figure 2, Table IV). Assignment of the two ortho hydrogen resonances in Figure 2 is based upon the fact that in $[Ni(S\text{-}p\text{-}C_6H_4Cl)_4]^{2-}$, two equivalent ortho hydrogens appear at −1.91 ppm.

In all the ^1H NMR spectra recorded so far, weak resonances around −7 ppm due to thiolato H atoms were observed (Figure 2). These signals were present even in the spectra of fresh (run within 5 min after dissolution) solutions of highly crystalline analytically pure compounds. The intensities of the resonances in the diamagnetic region did not change significantly with time. However, the relative ratio of the paramagnetic and diamagnetic thiolate signals was found to depend to a small extent on the initial concentration of the compounds. These weak diamagnetic thiolato ^1H signals in the NMR spectra of $[Ni(SAr)_4]^{2-}$ might arise from small amounts of diamagnetic ($S = 0$) planar nickel complex(es), which could be in equilibrium with the paramagnetic ($S = 1$) distorted-tetrahedral species (vide infra) provided that the time for the initial equilibration is very short and the rate of interconversion is far too slow as compared to the NMR time scale. The peak positions reported in Table IV have been checked in at least five independent runs with 15–30 mM solutions and were found to be within ±0.05 ppm at 298 k. We believe that the recorded peak positions are the values for a single species rather than averaged values for tetrahedral and square-planar species.

Magnetic susceptibility measurements in solution for the arenethiolates of nickel are beset by problems of concentration, solvent, and unusual temperature dependence. Previous attempts[2a] reported similar observations. Measurements with CD_3CN so-

(25) Swenson, D. Ph.D. Thesis, University of Iowa, 1979.
(26) Drago, R. S. In *Physical Methods in Chemistry*; Saunders: Philadelphia, 1977; Chapter 12.
(27) Horrocks, W. D., Jr. In *NMR of Paramagnetic Molecules: Principles and Applications*; La Mar, G. N., Horrocks, W. D., Holm, R. H., Eds.; Academic: New York, 1973; Chapter 4.

lutions in the concentration range 15–30 mM gave μ_{eff} of 2.7–2.9 μ_B at 298 K. Similar experiments in $(CD_3)_2SO$ yielded μ_{eff} values in the range 2.5–3.0 μ_B. These values are low for tetrahedral Ni(II) compounds. The low magnetic moment in solution of bis(iminobis(phosphine sulfido))nickel(II) (**3**) has been attributed to tetrahedral ($S = 1$) $\rightleftarrows$ planar ($S = 0$) equilibrium.[23] The temperature dependence of the solution magnetic susceptibility of the iminobis(phosphine sulfido) complex **3** indicated the diamagnetic planar species to be the favored one at lower temperatures. Since at a particular temperature, μ_{eff} values for the arenethiolates are found to be lower in more dilute (1–3 mM) solutions, it appears that the equilibrium is shifted toward the planar side even with dilution. Another possibility is polymerization into diamagnetic planar species like $[Ni_n(SAr)_{2(n+1)}]^{2-}$,[3b] following dissociation of coordinated thiolates from the paramagnetic distorted tetrahedral $[Ni(SAr)_4]^{2-}$. This possibility might also explain the appearance of weak thiolate peaks at −7 to −8 ppm in the NMR spectra of these complexes. However, addition of excess $(Et_4N)(SAr)$ to solutons of $[Ni(SAr)_4]^{2-}$ brought about hardly any change in the paramagnetically shifted resonance positions of the thiolate hydrogens reported in Table IV. This observation rules out the possibility of any equilibrium between diamagnetic multinuclear planar species and paramagnetic distorted-tetrahedral $[Ni(SAr)_4]^{2-}$ in solution. The reason(s) for lowering of μ_{eff} with dilution thus remains unclear.

The absorption spectra of 15–30 mM solutions of the complexes in acetonitrile exhibit a broad band with λ_{max} at 1800–1820 nm, a weak ($\epsilon \sim 20$ cm^{-1} M^{-1}) feature around 1280 nm and a strong absorption ($\epsilon = 650$–800 cm^{-1} M^{-1}) in the 660–680-nm region. These d–d bands are followed by intense charge-transfer bands in the 300–500-nm range. The intensity of the ~670-nm band is enhanced by overlap with high-energy charge-transfer absorption. Contrary to a previous report,[2a] extinction coefficients of the ~1800-nm band were found to be 70–120 cm^{-1} M^{-1} for fresh solutions of $[Ni(SAr)_4]^{2-}$ with no externally added thiolate. The ~1800-nm band has been assigned to $^3T_1 \rightarrow {}^3A_2$ ligand field transition of tetrahedral Ni(II).[2a,23] Thus the predominant Ni(II) species in the concentration range of NMR and magnetic susceptibility measurements is tetrahedral. The extinction coefficients of the d–d bands were found to decrease with time and on dilution. No attempt was made either to completely assign the electronic spectrum or to follow up the changes in extinction coefficients on dilution.

Summary

The following are the principal results and conclusions of this investigation.

(i) A high-yield straightforward synthetic route to tetraalkyl- and tetraarylammonium tetrakis(arenethiolato)nickelate(II) has been discovered.

(ii) The structure of $[Ni(S\text{-}p\text{-}C_6H_4Cl)_4]^{2-}$ has been determined. This structure along with the other reported briefly in a previous account demonstrates that, in $[Ni(SAr)_4]^{2-}$, the four arenethiolate ligands are arranged in a distorted tetrahedral manner. Two S–Ni–S angles are ~90° while the other four are close to 120°. Three of the four phenyl rings are coplanar with the corresponding Ni–S bonds.

(iii) On steric grounds, idealized square-planar or tetrahedral geometry for $[Ni(SAr)_4]^{2-}$ is not compatible with the tendency of the Ni–S vectors to be coplanar with the bonded phenyl rings. The observed distortion occurs to reduce steric interactions while maintaining coplanarity of Ni–S vectors and the phenyl rings. The previous suggestion of crystal packing force as the origin of such distortion seems to be highly unlikely.

(iv) The NMR spectra of several nickel arenethiolate complexes have been measured and assigned. The utility of ^1H NMR in probing paramagnetic thiolate-ligated Ni(II) sites in biological systems is apparent in the well-resolved, relatively narrow resonances exhibited by the complexes studied.

Acknowledgment. This research was supported by a Faculty Research Committee Grant at the University of California, Santa Cruz. We thank S. Swedberg for help in the initial synthetic attempts and Dr. F. Hollander for experimental assistance in crystal structure determination.

Registry No. **1**, 103003-19-6; $(Et_4N)_2[Ni(SC_6H_5)_4]$, 93841-89-5; $(Ph_4P)_2[Ni(SC_6H_5)_4]$, 57927-74-9; $(Et_4N)_2[Ni(S\text{-}m\text{-}C_6H_4Cl)_4]$, 103024-60-8; $(Et_4N)_2[Ni(S\text{-}p\text{-}C_6H_4CH_3)_4]$, 103003-21-0; $(Et_4N)_2NiCl_4$, 5964-71-6.

Supplementary Material Available: Thermal parameters of cations and the anion (Table S1) and positional and thermal parameters for hydrogen atoms of $(Et_4N)_2[Ni(S\text{-}p\text{-}C_6H_4Cl)_4]$ (Table S2) (4 pages). Ordering information is given on any current masthead page.

Contribution from the Department of Applied Chemistry, Faculty of Engineering, Osaka University, Suita, Osaka 565, Japan

Assimilatory and Dissimilatory Reduction of NO_3^- and NO_2^- with an $(n\text{-}Bu_4N)_3[Mo_2Fe_6S_8(SPh)_9]$ Modified Glassy-Carbon Electrode in Water

Susumu Kuwabata, Satoshi Uezumi, Koji Tanaka, and Toshio Tanaka*

Received January 2, 1986

The catalytic reduction of NO_3^- to NH_3 with an $(n\text{-}Bu_4N)_3[Mo_2Fe_6S_8(SPh)_9]$ modified glassy-carbon ([Mo-Fe]/GC) electrode has been accomplished for the first time by the controlled-potential electrolysis at −1.25 V vs. SCE in water. The current efficiency for the formation of NH_3 is 80.3% at pH 10. Not only NO_2^- but also NH_2OH were detected as reaction intermediates, and both of them are reduced to NH_3 quite easily under the same conditions. On the other hand, the reduction of NO_2^- with the same electrode at −1.10 V vs. SCE results in the evolution of N_2O without producing NH_3. Thus, the assimilatory reductions of NO_3^- and NO_2^- giving NH_3 take place when both substrates are reduced with the [Mo-Fe]/GC electrode at −1.25 V vs. SCE, whereas the dissimilatory reduction of NO_2^- affording N_2O selectively occurs in the electrochemical reduction of NO_2^- conducted at −1.10 V vs. SCE.

Introduction

The amounts of N_2, NH_3, NO_2^-, and NO_3^- in the natural world have been regulated by the nitrogen cycle (Scheme I).[1,2] Among those inorganic nitrogen molecules, only ammonia can be converted into organic nitrogen molecules in the metabolisms. Most of the higher plants and microorganisms that are not provided with the ability of N_2 fixation, therefore, reduce NO_3^- and NO_2^- to produce NH_3 (assimilatory reductions).[3] On the other hand, various denitrification bacteria reduce NO_3^- and NO_2^- to N_2O, which is further reduced to N_2 (dissimilatory reductions).[3-7] The latter

(1) Hughes, M. N. *The Inorganic Chemistry of Biological Processes*; Wiley: New York, 1981.
(2) Doelle, H. W. *Bacterial Metabolism*; Academic: New York, 1969.
(3) Payne, W. J. *Bacteriol. Rev.* **1973**, *409*, 1973 and references therein.

0020-1669/86/1325-3018$01.50/0